Dissection of Multibeam Satellite Communications with a Large-scale Antenna System Toolbox

Jesus Arnau and Carlos Mosquera
Signal Theory and Communications Department, University of Vigo - 36310 Vigo, Spain
{suso,mosquera}@gts.uvigo.es

***Abstract*—Current multibeam satellite systems consist of a very large number of spot beams. In this paper, we analyze them from the large scale MIMO perspective, and establish a comparison with massive MIMO systems. It will be shown that the large number of beams has important operational implications, and that it simplifies the analysis because it allows using asymptotic results. However, it will also be shown that current multibeam satellite links, despite their large number of antennas, do not qualify as massive MIMO systems.**

***Index Terms*—Multibeam satellites; large-scale analysis; Massive MIMO; multiuser detection.**

I. Introduction

Nowadays, multibeam satellite systems usually consist of a large number of spot beams, in an effort to serve large geographical areas with good performance. In the broader field of wireless communications, systems with many terminals and many antennas at the base station have been extensively studied, and with increasing interest [1]. Exploiting the large dimensions of such systems allows averaging out many undesired effects, and simplifies the analysis by resorting to random matrix theory (RMT) results and different central limit theorems.

A particular form of large-scale multiuser MIMO that has recently attracted a lot of attention is called *massive MIMO* [2]. Massive MIMO systems present an excess number of antennas at the base station, giving rise to a particular operation condition under which multiuser interference and noise have a minor impact, even with plain linear receivers.

In multibeam satellite communications, the large number of antennas and terminals has been extensively exploited for simplifying the analysis (see [3]–[5] and references therein), but this does not mean that multibeam satellites' performance scales with the number of antennas and terminals as terrestrial systems do.

In this work, we try to understand to which extent multibeam satellites qualify as large-scale antenna systems. We start by summarizing the most relevant characteristics of massive MIMO. We then describe the usual multibeam satellite return link [3], [6]–[8], for which we express some performance metrics in the large antenna regime; comparing these results with those from the massive MIMO literature, we will show that, even though most of the features of massive MIMO are not present in multibeam satellites, it is still possible to exploit the large dimensionality of the system to study its performance. The final comparison will address the acquisition of CSI both for the forward and return links.

The remaining of the document is structured as follows: Section II explains briefly the concept of massive MIMO, Section III describes multibeam satellite systems in comparison with massive MIMO systems, Section IV focuses on the problem of CSI acquisition, and finally Section V reports the conclusions of the paper.

II. Massive MIMO in a nutshell

Massive MIMO is a type of cellular multiuser MIMO in which the number of antennas at the base station is much larger than the number of terminals [9]. It is an instrument to synthesize extreme directivity (very high spatial resolution) in terrestrial cellular systems, giving rise to high multiplexing gains. The use of a large number of antennas, and the assumption of uncorrelation among them, provide SNR gain. Under certain propagation conditions, either in high scattering environments or under line-of-sight propagation conditions, such systems render almost-orthogonal channels among users, and very simple linear processing is optimal. In the following paragraphs, we will explain their most relevant characteristics.

A. Signal model

To explain the features above, consider a single cell with K terminals served by a single N-antenna base station. The received signal at the base station can be expressed as

$$\mathbf{y} = \sqrt{\gamma_{\mathrm{r}}}\mathbf{H}\mathbf{s} + \mathbf{n} \tag{1}$$

where $\mathbf{H} \in \mathcal{C}^{N\times K}$ is the matrix of channel coefficients, $\mathbf{s}$ is the unitary-power vector of transmitted symbols and $\mathbf{n}$ contains the noise samples, $\mathbf{n} \sim \mathcal{CN}(0, \mathbf{I})$. Here we assume that γ_{r} is the normalized signal-to-noise ratio (SNR), so that the rest of the variables can be assumed unit-power when needed.

In the massive MIMO literature, $\mathbf{H}$ is usually assumed to follow $\mathbf{H} = \mathbf{G}\mathbf{D}$, where $\mathbf{G}$ contains the fast fading coefficients $g_{ij} \sim \mathcal{CN}(0, 1)$ and $\mathbf{D}$ is a diagonal matrix comprising the large-scale fading (shadowing) effects.

Work supported by the Spanish Government under projects DYNACS (TEC2010-21245-C02- 02/TCM) and COMONSENS (CONSOLIDERINGENIO 2010 CSD2008-00010), and the Atlantic Research Center for Information and Communication Technologies (AtlantTIC).

B. Favorable propagation

In the massive MIMO context, favorable propagation occurs when the fast fading channels from the different users become almost orthogonal as the number of base station antennas grows large while keeping the number of terminals fixed [2], [10]. In other words, letting $\mathbf{g}_\ell$ denote the ℓ-th column of $\mathbf{G}$ –and thus the fast fading coefficients associated with the ℓ-th user–, if we define the ratio

$$\alpha \doteq N/K, \tag{2}$$

then

$$\lim_{\alpha\to\infty} \mathbf{g}_\ell^H \mathbf{g}_j \approx \begin{cases} N & \text{if } \ell = j, \\ 0 & \text{if } \ell \neq j. \end{cases} \tag{3}$$

The sum rate in the corresponding MU-MIMO return link is given by [2], [11]

$$\begin{aligned} C_{\text{sum}} &= \log_2 \det\left(\mathbf{I} + \gamma_{\text{r}} \mathbf{H}^H \mathbf{H}\right) \\ &\approx \sum_{\ell=1}^{K} \log_2\left(1 + N\gamma_{\text{r}} d_{\ell\ell}^2\right) \quad \text{bps/Hz} \end{aligned} \tag{4}$$

where $d_{\ell\ell}$ denotes the ℓ-th element in the diagonal of $\mathbf{D}$; we can see that the maximum performance achievable is the same as in an interference-free system impaired by shadowing.

Similar considerations can be made for line-of-sight channels: as N grows, the angular resolution of the antenna array increases so users can be separated more effectively by the appropriate antenna weights.

C. Performance of linear detection

A crucial consequence of favorable propagation is that very simple linear receivers are almost optimum: consider that the base station has perfect knowledge of $\mathbf{G}$ but ignores $\mathbf{D}$, and that it applies matched filtering to the received signal. Then,

$$\hat{\mathbf{s}} = \mathbf{G}^H \mathbf{y} \approx N\sqrt{\gamma_{\text{r}}}\mathbf{D}\mathbf{s} + \mathbf{G}^H \mathbf{n}, \tag{5}$$

and the SINR experienced by the ℓ-th user is

$$\text{sinr}_\ell \approx \frac{\gamma_{\text{r}} N^2 d_{\ell\ell}^2}{\mathbb{E}\left[(\mathbf{g}_\ell^H \mathbf{n})^2\right]} = N\gamma_{\text{r}} d_{\ell\ell}^2 \tag{6}$$

which is the SINR that renders the optimum rate (4).[1]

D. Limitations

Exploiting the potential of massive MIMO requires obtaining an accurate estimation of $\mathbf{G}$, and then exploiting it, all during the coherence time of the channel. This constrains the length of the pilot sequences and, in consequence, their cardinality.

In this respect, and as currently formulated, massive MIMO would require time division duplex communication and channel reciprocity to partially overcome this problem. In this way, the forward link transmission could simply use the channel estimation obtained from return link pilots.

[1]The corresponding expressions under channel estimation error can be found in [2, Table I].

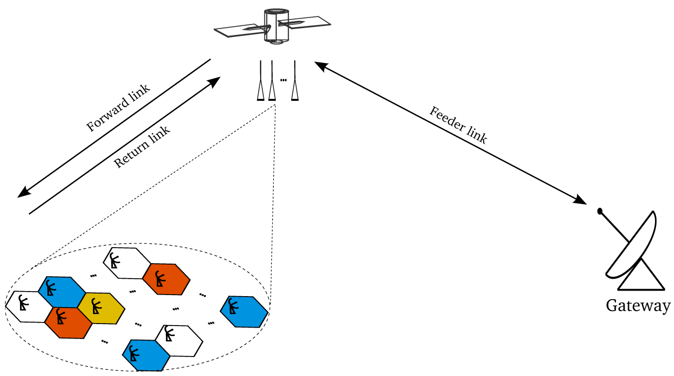

Figure 1. A multibeam satellite architecture.

Also, the problem of assigning pilot sequences to terminals becomes more complicated when cells nearby use the same frequency band. In this case, if terminals in different cells use the same sequence, then the corresponding channel estimations will be altered, a phenomenon called *pilot contamination*.

Other possible limitations of massive MIMO [12] include space constraints at the base station, channel aging and reduced degrees of freedom because of spatial correlation.

III. Large Scale Multibeam Satellite Systems

In this section we will explain the features of large scale multibeam satellite systems, comparing each aspect with that in massive MIMO systems; a final comparison pertaining CSI acquisition in both cases will be addressed in Section IV.

A. Signal model

We will focus on a multibeam channel with K single-antenna terminals transmitting towards a single satellite equipped with N antennas (Figure 1); some forward link considerations will follow in Section IV. The signal model is

$$\mathbf{y} = \sqrt{\gamma}\mathbf{H}\mathbf{s} + \mathbf{n} \tag{7}$$

where $\mathbf{s} \in \mathcal{C}^{K\times 1}$ is the transmitted signal vector, $\mathbb{E}\left[\mathbf{s}\mathbf{s}^H\right] = \mathbf{I}$, $\mathbf{y} \in \mathcal{C}^{N\times 1}$ is the received signal vector at the gateway, assuming a transparent feeder link, $\mathbf{n} \sim \mathcal{CN}(\mathbf{0}, \mathbf{\Sigma})$ is the complex noise vector and γ is the normalized SNR.

Matrix $\mathbf{H} \in \mathcal{C}^{N\times K}$ represents the complex-valued channel and can be expressed as [3], [5], [7]

$$\mathbf{H} = \mathbf{G}\mathbf{D}. \tag{8}$$

Despite the obvious similarity with the terrestrial massive MIMO case, both channel models are quite different. Here, $\mathbf{G} \in \mathcal{C}^{N\times K}$ is a full column-rank matrix containing the antenna radiation pattern, and $\mathbf{D} \in \mathcal{C}^{K\times K}$ denotes a diagonal matrix of random entries modeling the propagation effects. In particular, $\mathbf{G}$ in (8) accounts for the on-board antenna responses and the fixed weighting matrix. Planar phased-array antennas are a common technology for LEO and MEO satellites, whereas aperture antennas with multiple feeds are the usual solution for GEO satellites. The large number of radiators synthesize very directive beams, which in most cases

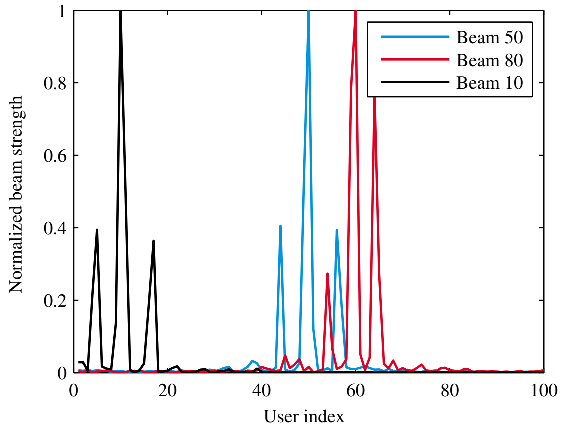

Figure 2. Beam pattern example, provided by ESA in the framework of [15].

are fixed, precluding the use of advanced signal multiuser processing. For those few cases for which adaptive weights are implemented, either on-board or on-ground, technological constraints impose tight limits on the number of radiating elements and, in consequence, on the achievability of the "massive" regime.

Multiuser satellite channels exhibit *diagonal fading*, that is, all the channel coefficients from one user to the different antenna elements are the same. This is caused by the relatively small separation of the antenna elements compared with the satellite altitude. The corresponding values are included in the diagonal matrix $\mathbf{D}$ in (8); a similar diagonal matrix in the terrestrial model contains the large-scale fading effects. The statistical model of the fading coefficients depends on the frequency band and type of service [13].

B. (Un)Favorable propagation

Asymptotic orthogonality between channel vectors associated with different terminals is behind the high multiplexing gain in massive MIMO systems, for both highly isotropic and line-of-sight channels [10]. For finite dimensions, the columns of the matrix $\mathbf{G}$ in (8) are not orthogonal. As an illustration, Figure 2 depicts the normalized radiation pattern of three different beams –from a total of 100 beams and 155 feeds– taken from [6], [14]. A direct consequence of this lack of orthogonality leading to significant multiuser interference, is that linear receivers may be far from optimum. Indeed, [14] and [8] independently report substantial differences between linear and non-linear detection.

Without orthogonality, the sum rate of the return link, given by

$$\begin{aligned} C_{\text{sum}} &= \log_2 \det \left(\mathbf{I} + \gamma \mathbf{D}^2 \mathbf{G}^H \mathbf{G} \right) \\ &= \sum_{\ell=1}^{K} \log_2 \left(1 + \gamma \lambda_\ell \left\{ \mathbf{D}^2 \mathbf{G}^H \mathbf{G} \right\} \right) \end{aligned} \tag{9}$$

with $\lambda_\ell\{\}$ the ℓ-th largest eigenvalue of a matrix, is difficult to characterize. Yet, the involved large dimensions make it possible to obtain some asymptotic results as detailed next.

C. Performance analysis in the large antenna regime

When both N and K tend to infinity, the sum rate approaches

$$\begin{aligned} \lim_{N,K\to\infty} C_{\text{sum}} &= \lim_{N,K\to\infty} \sum_{\ell=1}^{K} \log_2 \left(1 + \gamma \lambda_\ell \left\{ \mathbf{D}^2 \mathbf{G}^H \mathbf{G} \right\} \right) \\ &= K \mathbb{E}_{\mathbf{D}} \left[\log_2 \left(1 + \gamma \lambda \left\{ \mathbf{D}^2 \mathbf{G}^H \mathbf{G} \right\} \right) \right] \\ &= K \int \log_2 \left(1 + \gamma x \right) \, \mathrm{d}F_{\mathbf{D}^2 \mathbf{G}^H \mathbf{G}}(x) \end{aligned} \tag{10}$$

where $F_{\mathbf{D}^2\mathbf{G}^H\mathbf{G}}(x)$ is the cumulative distribution function (CDF) of the eigenvalues of matrix $\mathbf{D}^2\mathbf{G}^H\mathbf{G}$. We have that C_{sum} converges to a deterministic value, as illustrated in Figure 3, which shows different realizations of $1/\tilde{K} \cdot \log\det\left(\mathbf{I} + \gamma \tilde{\mathbf{H}}^H \tilde{\mathbf{H}}\right)$ as a function of γ. $\tilde{\mathbf{H}}$ are square submatrices of $\mathbf{H}$, the channel matrix used in [5], [14], [15], of length $\tilde{K}$. We can see that the depicted quantity tends to be deterministic as $\tilde{K}$ grows large.

Solving (10) in closed form is in general very difficult, as it requires knowing the distribution of the eigenvalues of a matrix with random entries. RMT has played a crucial role in providing solutions to this problem when the dimensions of the system are large: not only the instantaneous sum rate can be expressed as an average (since we are, in fact, averaging over a large number of users and antennas), but also the empirical density of the eigenvalues converges to a deterministic function in many cases.

Unfortunately, convergence of the empirical distribution does not guarantee that it will be easy to obtain or to manipulate. Often, the limiting spectral function is obtained through a *transform* of its function. The authors in [16], for example, obtained directly the Shannon transform[2] of the empirical eigenvalues of a matrix product similar to $\mathbf{D}^2\mathbf{G}^H\mathbf{G}$, although the resulting expressions are still quite involved.

An alternative line of research is that of obtaining tight bounds, or high and low SNR approximations, exploiting the large dimensionality of the system [4], [5], [7]. In the following, we will reproduce some high SNR results, illustrating how environmental fading does not vanish in this case.

At high SNR, capacity can be approximated by

$$\begin{aligned} C_{\text{sum}} &\approx \log_2 \det \left(\gamma \mathbf{G}^H \mathbf{G} \right) + \sum_{\ell=1}^{K} \log_2 d_{\ell\ell}^2 \\ &\xrightarrow{K\to\infty} \log_2 \det \left(\gamma \mathbf{G}^H \mathbf{G} \right) + K \mathbb{E} \left[\log_2 d_{\ell\ell}^2 \right] \end{aligned} \tag{11}$$

when the elements $d_{\ell\ell}$ are i.i.d. Since $d_{\ell\ell}$ take values between 0 and 1, the expectation above will take negative values; it is thus clear that fading is detrimental to performance, and that the large dimensionality of the system does not make this effect disappear. The right-hand summation in (11) converges

[2]For any nonnegative random variable X, this transform is defined as $\mathcal{V}_X(\gamma) \doteq \mathbb{E}\left[\log(1+\gamma X)\right]$ [17].

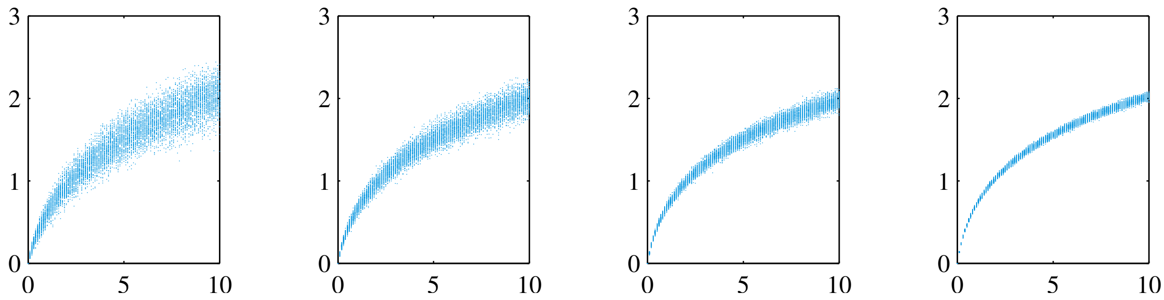

Figure 3. Realizations of $1/\tilde{K} \cdot \log\det\left(\mathbf{I} + \gamma\tilde{\mathbf{H}}^H\tilde{\mathbf{H}}\right)$ as a function of γ; from left to right, $\tilde{K} = \{3, 7, 19, 100\}$.

for large K to a random variable with known distribution, usually Gaussian, with a variance decreasing with K. This holds under mild assumptions which do not necessarily require independence. In consequence, the outage capacity benefits from this large dimensionality.

D. Technological limitations

Some communication satellites currently in orbit fly large antenna arrays. As an example for mobile links, consider the Globalstar phased-array transmit antenna at 2.5 GHz (91 antennas, 16 beams) or the Iridium 3 phased-array antennas for the mobile link, each with 106 elements, planar antennas in both cases [13]. High numbers of antennas can be found also in some modern multibeam GEO satellites.

The two main gains of massive MIMO systems, namely, multiplexing and SNR, comes from the use of such a large number of antennas that the multiuser interference is negligible, and the equivalent antenna gain is so high that the noise impact is small compared to the difficulties when estimating such a large number of channels.

In order to reap the massive MIMO promised benefits, satellites would need to increase substantially the picked power and to improve the ability to differentiate the user signals through the increase of the number of antennas without necessarily avoiding the use of the same frequency channels in adjacent beams. In short, the resulting increased aperture antenna would collect more power, whereas a simple matched filter would provide multiplexing gain. Similar considerations apply for the forward link.

Even though terrestrial systems can conceive the use of very large antenna arrays at base stations, the technogical barriers in satellites would prevent a significant increase in the number of radiating elements with respect to current technology: not only much larger antennas would be needed, but also the requirements in terms of on-board power amplifiers and feeder link bandwidth would become unfeasible.

IV. Acquiring CSI at the Receiving End

As outlined in Section II-D, obtaining CSI at the base station is among the most challenging tasks in massive MIMO systems. The training sequence length scales with the number of terminals in the return link, but with the number of base station antennas in the forward link, which is considered impractical[3]. For this reason, the massive MIMO literature advocates for the use of Time Division Duplexing (TDD), exploiting channel reciprocity to use the return channel estimates for both forward and return directions. It is worth noticing that perfect timing and frequency synchronization is usually assumed, thus simplifying the estimation process. Satellite links employ different frequencies for the uplink and downlinks, so channel reciprocity cannot be exploited, at least up to the point required by multiuser signal processing schemes. Some studies have been conducted to exploit the estimated channel for the reverse direction, although the results are still preliminary [18], [19]. Therefore, channel estimation is needed in both directions as explained next.

A. Estimation in the forward link

Assume that a distinct sequence of length L symbols is sent through each antenna element. Then, the set of signals received by the terminals can be expressed as

$$\mathbf{Y} = \sqrt{\gamma_{\mathrm{FL}}}\mathbf{H}_{\mathrm{FL}}\mathbf{C} + \mathbf{N} \tag{12}$$

where $\mathbf{H}_{\mathrm{FL}} \in \mathcal{C}^{K\times N}$ is the forward link channel matrix, $\mathbf{Y} \in \mathcal{C}^{K\times L}$ is the stack of received sequences (one at each terminal), $\mathbf{C} \in \mathcal{C}^{N\times L}$ is the stack of transmitted sequences and $\mathbf{N} \in \mathcal{C}^{K\times N}$ contains the additive noise samples.

A common estimation technique is the least squares method [20], which in this case coincides with the maximum likelihood solution and is given by

$$\hat{\mathbf{H}}_{\mathrm{FL}} = \mathbf{Y}\mathbf{C}^{\dagger} = \sqrt{\gamma_{\mathrm{FL}}}\mathbf{H}_{\mathrm{FL}} + \mathbf{N}\mathbf{C}^{\dagger} \tag{13}$$

where $\mathbf{C}^{\dagger}$ is the (right-hand side) pseudoinverse of $\mathbf{C}$; this pseudoinverse will exist if $\mathbf{C}$ has full rank, and thus $L \geq N$ is a necessary condition. As proven among others in [20], orthogonal sequences minimize the mean squared estimation error, and thus Walsh-Hadamard sequences constitute a popular choice.

The long roundtrip time in a satellite communication is a drawback for adaptation in mobile links, since the channel coherence might be shorter than the time it takes to the channel

[3] An added problem in the forward link case is that, once the terminals compute the estimates, they have to feed quantized versions of them back to the station; the higher accuracy is required, the higher return link capacity is demanded in this process.

estimates to make it back to the transmit side for proper precoding. On the other hand, this is not considered to be a major problem in fixed satellite communications operating at the K band (or above).

B. Estimation in the return link

Similarly to the forward link case, the transmission of pilot sequences in the return link can be expressed as

$$\mathbf{Y} = \sqrt{\gamma}\mathbf{H}\mathbf{C} + \mathbf{N}, \tag{14}$$

with $\mathbf{C}$ a matrix of size $K \times L$; as opposed to the forward link, it suffices to fulfill $L \geq K$.

One of the complications when estimating the return link responses is the lack of synchronism at the receive side among the signals coming from different users, giving rise to time and and frequency errors. As a consequence, at a given time instant t, the signal received corresponding to the ℓ-th training sequence will not be $c_\ell(t)$, but [8]

$$c_\ell(t+\tau)e^{j\omega_\ell t+\theta_\ell}. \tag{15}$$

Sampling the above sequences at symbol period would produce the matrix $\mathbf{C}$, whose entries are not perfectly known unless τ, ω and θ are known. Different timing and frequency recovery techniques have been tested specifically for multi-beam return links using multiuser detection [21]. The latter reference proposed a hybrid algorithm, where a non-data aided estimate is refined by exploiting the pilot pattern, and concluded that good performance results can be obtained if the start of the frames can be correctly decoded, even though better pilot sequences would probably be required.

However, even when $\mathbf{C}$ is known, the properties of the original discrete-time sequences may be lost: starting from a vector of length L, $\mathbf{c}_\ell = (c_{\ell 1}\ c_{\ell 2}\ \cdots\ c_{\ell L})$, we have that

$$c_\ell(t) = \sum_{k=1}^{L} c_{\ell k}\, g(t-kT) \tag{16}$$

where $g(t)$ is the transmit pulse and T the symbol period. With no timing or frequency errors, sampling the signal above would return the original sequence (this was the case in the forward link), but otherwise a sequence with very different properties might be obtained. For this reason, [8] proposes pseudo-random sequences instead of Walsh-Hadamard sequences, trying to preserve performance even when orthogonality is lost.

If orthogonality can be assumed between the sequences, the resulting estimate can be written as $\hat{\mathbf{H}} = \mathbf{H} + \mathbf{E}$, where $\mathbf{E}$ is a random error matrix; this is the usual model for forward link channel estimation, and also the return link simplification adopted among others in [8]. In [22] the error after MMSE detection was studied for any deterministic matrix $\mathbf{H}$ and error matrices satisfying some mild assumptions. Analytical results for the medium and high SNR regimes were found, once again through RMT results, revealing that the error converges to a deterministic value as K grows large, and that such value can be obtained by solving a system of $2K$ equations.

The case with pseudo-random sequences is more complicated. In this case, and even at high SNR, imperfect estimation results into an interference floor which cannot be removed. An expression for the asymptotic SNR of a user after MMSE detection is given in [14], showing that it depends only on the characteristics of the sequences; the numerical results therein showed a throughput cutoff by one half with respect to the perfect CSI case when using training sequences of length $1,000$. Focusing on the estimation error itself, such floor was quantified in [23] for different types of sequences.

Finally, pilot contamination, a pivotal concept in massive MIMO systems, is not an issue here as long as there is only one satellite (analogous to a single base station). Such effect could appear, however, for very large coverages with multiple satellites and independent processing of their signals.

V. Conclusions

Current multibeam satellites employ a large number of antennas, even a few hundreds, to cover large extensions with different beams. This is not the case for wireless terrestrial base stations, which use a few antennas at most for coverage of regions comparably much smaller. Recent research advocates for the concentration of many antennas on the same site so as to reduce the multiuser interference, increase the SNR and simplify the signal processing thanks to some asymptotic MU-MIMO properties. Although it is still an open debate whether the required installations, which definitely would require larger radiating surfaces, are a cost effective solution, we have made some initial considerations for the satellite user links. Asymptotic tools such as random matrix theory and central limit theorems can be used to obtain some capacity results. However, it is not realistic to consider that noise and/or interference are not the limiting factors: given the high involved propagation distances, the required effective area of the satellite antennas would need to grow considerably, beyond current technology. There is no channel reciprocity either, but fortunately channel estimation does not suffer from pilot contamination in the return link (unless more than one satellite is used).

As future work it will be important to understand the number of antennas in different settings for which linear processing matches non-linear schemes, and also when simple schemes such as beamforming/matched filtering compare to more complex zero-forcing/MMSE, respectively.

Appendix A
Why diagonal fading

Diagonal fading, as understood through this work, appears when all the receiving elements experience the same fading coefficient. For satellite channels, this model can be easily derived following the lines of [7]. Start by considering

$$\mathbf{H} = \mathbf{G} \odot \mathbf{F} \tag{17}$$

with $\mathbf{G}$ the antenna pattern matrix and $\odot$ the entry-wise product, such that each element of the antenna pattern would be scaled by the corresponding fading coefficient in matrix $\mathbf{F}$.

Table I

SUMMARY OF THE COMPARISON BETWEEN MASSIVE MIMO AND A MULTIBEAM SATELLITE SYSTEM

	Massive MIMO	Multibeam Sat.
Channel model	$\mathbf{H} = \mathbf{GD}$	$\mathbf{H} = \mathbf{GD}$
$\mathbf{G}$	Random fading columns	Antenna pattern
$\mathbf{D}$	Random shadowing	Random fading
Excess antennas at BS	Yes	Probably no
Favorable propagation	Yes	No
Optimum receiver (RL)	MF	MMSE-SIC
Sum rate (RL)	$\sum \log_2 \left(1 + N\gamma_r d_{\ell\ell}^2\right)$	$\sum \log_2 \left(1 + \gamma\lambda_\ell \left\{\mathbf{D}^2\mathbf{G}^H\mathbf{G}\right\}\right)$
RMT applies	Yes	Yes
Channel reciprocity	Probably yes	No
Pilot contamination	Yes	No (single Sat.).

Assume now the common Kronecker correlation model, so that $\mathbf{F} = \mathbf{R}_{\text{rx}}^{1/2}\tilde{\mathbf{F}}\mathbf{R}_{\text{tx}}^{1/2}$. If there is total correlation at the receiving end, then $\mathbf{F} = \mathbf{1}\tilde{\mathbf{F}}\mathbf{R}_{\text{tx}}^{1/2}$. The resulting rank-one matrix has constant columns. Since element-by-element multiplication by a matrix with constant columns is equivalent to scaling each column, we conclude that $\mathbf{H}$ can be expressed as $\mathbf{GD}$ with $\mathbf{D}$ a diagonal matrix.

REFERENCES

[1] "Large-scale multiple antenna wireless systems," *IEEE J. Sel. Areas Commun.*, no. 2, 2013.

[2] F. Rusek, D. Persson, E. G. Larsson, T. L. Marzetta, and F. Tufvesson, "Scaling up MIMO: Opportunities and challenges with very large arrays," *IEEE Signal Process. Mag.*, vol. 30, no. 1, pp. 40–60, Jan. 2013.

[3] N. Letzepis and A. J. Grant, "Capacity of the multiple spot beam satellite channel with rician fading," *IEEE Trans. Inf. Theory*, vol. 54, no. 11, pp. 5210–5222, Nov. 2008.

[4] D. Christopoulos, J. Arnau, S. Chatzinotas, C. Mosquera, and B. Ottersten, "MMSE performance analysis of generalized multibeam satellite channels," *IEEE Commun. Lett.*, vol. 17, no. 7, pp. 1332–1335, Jul. 2013.

[5] J. Arnau and C. Mosquera, "Performance analysis of multiuser detection for multibeam satellites under rain fading," in *Proc. ASMS & SPSC*, Baiona, Spain, Sep. 2012, pp. 212–219.

[6] J. Arnau, B. Devillers, C. Mosquera, and A. Pérez-Neira, "Performance study of multiuser interference mitigation schemes for hybrid broadband multibeam satellite architectures," *EURASIP J. Wirel. Commun. Netw.*, vol. 2012, no. 1, p. 132, Apr. 2012.

[7] D. Christopoulos, S. Chatzinotas, M. Matthaiou, and B. Ottersten, "Capacity analysis of multibeam joint decoding over composite satellite channels," in *Proc. ASILOMAR*, Pacific Grove, CA, Nov. 2011, pp. 1795–1799.

[8] M. Debbah, G. Gallinaro, R. Müller, R. Rinaldo, and A. Vernucci, "Interference mitigation for the reverse-link of interactive satellite networks," in *9th Int. Work. Signal Process. Sp. Commun.*, Sep. 2006.

[9] F. Boccardi, R. Heath, A. Lozano, T. Marzetta, and P. Popovski, "Five disruptive technology directions for 5G," *IEEE Commun. Mag.*, vol. 52, no. 2, pp. 74–80, February 2014.

[10] T. L. Marzetta, "Noncooperative cellular wireless with unlimited numbers of base station antennas," *IEEE Trans. Wireless Commun.*, vol. 9, no. 11, pp. 3590–3600, Nov. 2010.

[11] E. Telatar, "Capacity of multi-antenna gaussian channels," *Eur. Trans. Telecommun.*, vol. 10, no. 6, pp. 585–595, Nov. 1999.

[12] R. W. Heath Jr., "What is the role of MIMO in future cellular networks: Massive? coordinated? mmWave?" in *ICC Workshop Plenary Beyond LTE-A*, Budapest, Hungary., 2013. [Online]. Available: http://users.ece.utexas.edu/ rheath/presentations/2013/ Future_of_MIMO_Plenary_Heath.pdf

[13] M. W. E. Lutz and A. Jahn, *Satellite Systems for Personal and Broadband Communications*. Springer, 2000.

[14] J. Arnau-Yanez, M. Bergmann, E. A. Candreva, G. E. Corazza, R. de Gaudenzi, B. Devillers, W. Gappmair, F. Lombardo, C. Mosquera, A. Perez-Neira, I. Thibault, and A. Vanelli-Coralli, "Hybrid space-ground processing for high-capacity multi-beam satellite systems," in *Proc. GLOBECOM*, Houston,TX., Dec. 2011, pp. 1–6.

[15] "The SatNEx III Project." [Online]. Available: http://telecom.esa.int/telecom/www/object/index.cfm?fobjectid=30263

[16] N. Letzepis and A. Grant, "Shannon transform of certain matrix products," in *Proc. ISIT*, Nice, France, 2007, pp. 1646–1650.

[17] A. M. Tulino and S. Verdú, "Random matrix theory and wireless communications," *Found. Trends™ Commun. Inf. Theory*, vol. 1, no. 1, pp. 1–182, Jul. 2004.

[18] B. Hochwald and T. Marzetta, "Adapting a downlink array from uplink measurements," *IEEE Trans. Signal Process.*, vol. 49, no. 3, pp. 642–653, Mar. 2001.

[19] J. Arnau and C. Mosquera, "Open loop adaptive coding and modulation for mobile satellite return links," in *Proc. AIAA ICSSC*, Firenze, Italy, Oct. 2013.

[20] M. Biguesh and A. Gershman, "Training-based MIMO channel estimation: a study of estimator tradeoffs and optimal training signals," *IEEE Trans. Signal Process.*, vol. 54, no. 3, pp. 884–893, Mar. 2006.

[21] Z. Abu-Shaban, B. Shankar, D. Christopoulos, and P.-D. Arapoglou, "Timing and frequency synchronisation for multiuser detection on the return link of interactive mobile satellite networks," in *Proc. AIAA ICSSC*, Firenze, Italy., Oct. 2013.

[22] J. Arnau and C. Mosquera, "Multiuser detection performance in multibeam satellite links under imperfect CSI," in *Proc. ASILOMAR*, Pacific Grove, CA, Nov. 2012, pp. 468–472.

[23] M. Bergmann, W. Gappmair, C. Mosquera, and O. Koudelka, "Channel estimation on the forward link of multi-beam satellite systems," in *Personal Satellite Services*, ser. Lecture Notes of the Institute for Computer Sciences, Social Informatics and Telecommunications Engineering, G. Giambene and C. Sacchi, Eds. Springer Berlin Heidelberg, 2011, vol. 71, pp. 250–259.